



Structural and magnetic properties and hyperfine interaction in $\text{La}_{3.5}\text{Ru}_4\text{O}_{13}$ compound

J.A.H. Coaquira^{a,*}, L.B. Carvalho^b, R.L. de Almeida^b, A.W. Carbonari^c, G.A. Cabrera-Pasca^c, S. Quezado^b, S.K. Malik^b

^a Núcleo de Física Aplicada, Instituto de Física, Universidade de Brasília, Brasília, DF 70910-900, Brazil

^b International Center for Condensed Matter Physics, University of Brasília, Brasília, DF 70904-970, Brazil

^c Instituto de Pesquisas Energéticas e Nucleares, Comissão Nacional de Energia Nuclear, Centro do Reator de Pesquisas, Universidade de São Paulo, São Paulo, SP 05508-000, Brazil

ARTICLE INFO

Keywords:

Solid-state reaction
Ruthenates
Magnetization
PAC spectroscopy

ABSTRACT

Structural, magnetic and hyperfine interaction measurements have been carried out on the novel compound $\text{La}_{3.5}\text{Ru}_4\text{O}_{13}$ prepared under two different atmospheres (air and oxygen flow). This compound is formed in the orthorhombic structure (space group Pmmm, # 47). The coexistence of the triple-layered *perovskite-type* planes (quasi-2D structure) and the *rutile-like* slabs (1D structure) leads to interesting magnetic and electronic properties in this compound. The magnetic susceptibility of this system shows a peak at $T \sim 47$ K associated with antiferromagnetic interactions. The Curie–Weiss behaviour of the susceptibility provides an effective magnetic moment consistent with Ru ions in low-spin state. Perturbed angular correlation measurements carried out with ^{111}Cd probe in the temperature range 10–60 K reveal only quadrupole interactions and indicate the occurrence of structural distortions for $T < 40$ K.

© 2009 Elsevier B.V. All rights reserved.

1. Introduction

The ruthenates (4d transition-metal oxides) are one of the most intriguing systems and exhibit a variety of interesting properties such as unconventional superconductivity, as observed in Sr_2RuO_4 [1], high T_C (Curie temperature) ferromagnetism in $\text{Sr}_4\text{Ru}_3\text{O}_{10}$ [2], Fermi-liquid behaviour in $\text{La}_3\text{Ru}_3\text{O}_{11}$ [3], a non-Fermi-liquid behaviour in $\text{La}_4\text{Ru}_6\text{O}_{19}$ [4], etc. In some systems, such as La_2RuO_5 [5], the orbital ordering is expected to play a special role. The more extended nature of the 4d orbitals (relative to their 3d counterparts) is expected to considerably enhance the electron–lattice interaction, which seems to be the reason for the formation of a variety of structures and also should be the source of structural phase transitions caused by metal ion substitutions [6]. This higher degree of delocalization of 4d orbitals also tends to produce a greater overlap between them, leading to the decrease of the intra-ionic Coulomb interaction in 4d-metal oxides compared to that in the 3d counterparts [7].

In view of the interesting properties exhibited by Ruthenates, we have studied structural, magnetic and hyperfine properties of the novel $\text{La}_{3.5}\text{Ru}_4\text{O}_{13}$ compound and the results are presented and discussed here.

2. Experimental

Polycrystalline samples of $\text{La}_{3.5}\text{Ru}_4\text{O}_{13}$ were synthesized from lanthanum hydroxide $\text{La}(\text{OH})_3$ (99.9%) and RuO_2 (99.95%) using conventional solid-state reaction technique. Pellets were fired in air (sample S2) and under O_2 flow (sample S3) at 1100°C for ~ 48 h. Intermediate grindings were performed in order to ensure homogeneity of the samples. Sample preparation details are published elsewhere [8]. Crystal-structure characterization and phase determination were carried out by X-ray diffraction (XRD). Magnetic measurements were carried out using commercial SQUID and VSM magnetometers. Perturbed angular correlation (PAC) measurements were performed in the temperature range from 10 to 60 K using ^{111}In isotopes diffused into the sample.

3. Results and discussion

The XRD data analyses using the Rietveld method showed that both samples are single phase compounds, crystallizing in the orthorhombic structure (space group Pmmm, #47) [9]. Fig. 1 shows the fitted XRD pattern for sample S2. Lattice parameters determined from the fits are collected in Table 1.

The crystal structure of $\text{La}_{3.5}\text{Ru}_4\text{O}_{13}$ is formed by seven O sites and three sites for both La and Ru ions, with the latter exhibiting octahedral coordination [8]. The three Ru octahedra are

* Corresponding author. Tel.: +55 61 3307 2900; fax: +55 61 3307 2363.
E-mail address: coaquira@unb.br (J.A.H. Coaquira).

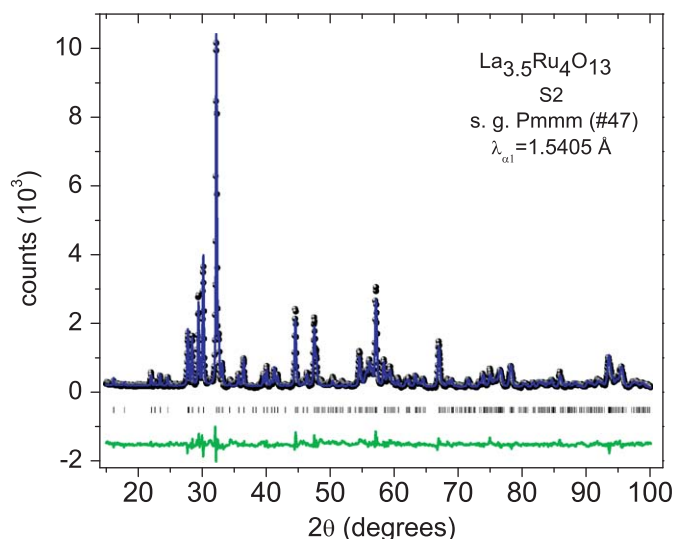


Fig. 1. XRD pattern of the samples S2 refined using the Rietveld method. Solid points are the data and line is the calculated curve. The difference between observed and calculated data is shown at the bottom part of the figure. Vertical marks represent the Bragg reflections.

Table 1

Collection of the structural parameters for $\text{La}_{3.5}\text{Ru}_4\text{O}_{13}$ compound prepared in air and under O_2 flow.

Parameter	S2 (on air)	S3 (on O_2)
a (Å)	11.9881 (3)	11.9934 (2)
b (Å)	5.6115 (1)	5.6124 (1)
c (Å)	3.8550 (1)	3.8557 (1)
Ru(1)–O (Å)	1.9929	1.9934
Ru(2)–O (Å)	1.9938	1.9944
Ru(3)–O (Å)	1.9796	1.9800

distributed in the following way: two of them, Ru(1) O_6 and Ru(2) O_6 are corner-shared through O atoms forming a triple-layered perovskite-type structure along the [100] direction with La ions (La(1) and La(2)) occupying the interstitial spaces. Ru(3) O_6 octahedra are edge-shared, thus forming one-dimensional (1D) slabs along the [010] direction similar to those formed in a rutile structure. More detailed description of this structure is found in Ref. [8]. Comparing the average Ru–O distances (see Table 1) of both samples, the sample prepared under oxygen flow shows slightly larger values. Both samples show similar average metal–oxygen bond distances for Ru(1) and Ru(2) ions, which suggest the same oxidation state for these two Ru ions forming the perovskite-type layers. However, the relatively shorter metal–oxygen bond distance for Ru(3) suggests stronger d–p orbital hybridization, which implies a different oxidation state for it. This finding appears to be reasonable since a careful examination of the 1D slabs reveals that the average Ru(3)–Ru(3) bond distance (~ 2.806 Å) is smaller than that in rutile crystal (3.107 Å). This smaller bond distance along the 1D slabs in the $\text{La}_{3.5}\text{Ru}_4\text{O}_{13}$ compound causes the delocalization of 4d-electrons along the b -axis reducing the bond length of Ru(3)–O and producing a fractional oxidation state for Ru(3) ions in agreement with the oxidation state expected for the nominal value (+3.5). These bond distances have been confirmed by preliminary neutron diffraction studies on this compound [10]. Similar behaviour of bond distances in this compound has been also reported by Abraham et al. [9].

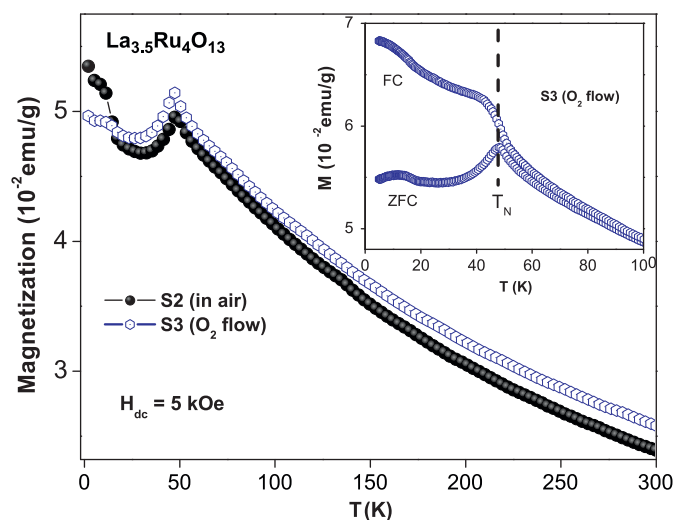


Fig. 2. M vs. T curves for both samples (S2 and S3). The inset shows the ZFC and FC curves of the S3 sample.

The oxidation state of Ru ions can be estimated by using the bond-valence method where the bond valence V_i is given by: $V_i = \sum_j \exp[(R_i - d_{ij})/b]$ where d_{ij} represents the bond length between Ru (i)-ion and oxygen (j) ion, R_i is the bond-valence parameter and b is a constant equal to 0.37 Å [11]. Using $R_i = 1.834$ Å (Ref. [11]) and the bond distances determined from the XRD analysis, a value of $\sim +4.0$ is estimated. The smaller valence state of +3.5 expected for Ru(3) drives one to expect a small bond-valence parameter value ($R_i \sim 1.78$ Å). A dependence of the bond-valence parameter on the oxidation state of metals bond to oxygen ions has been reported, which seems to increase with the oxidation state [11].

Fig. 2 shows the temperature (T) dependence of the magnetization (M) for both samples (S2 and S3), obtained in a field of $H = 0.5$ T. The M vs. T curve for the sample prepared under oxygen flow (S3) shows some remarkable features in the low-temperature region: a cusp centred at ~ 47 K, a shoulder centred at ~ 12 K and a modest increase when the temperature is further decreased below 12 K. The sample prepared in air (S2) shows the same features, although the increasing contribution at the lowest temperatures is more evident than that shown by the sample S3. Below the cusp, both samples show thermal irreversibility between the ZFC and FC curves (see inset of Fig. 2).

In the high-temperature region, the susceptibility is well described by the Curie–Weiss law. From the fit, we obtain an effective magnetic moment, $\mu_{\text{eff}} \sim 2.7 \mu_B$ per Ru ion and a Weiss temperature, $\theta = -260$ K for the sample S3. Smaller magnetic moment and a less negative θ are obtained for the sample prepared in air (S2). The negative value of θ indicates that antiferromagnetic (AFM) interactions are governing the magnetic state of Ru ions at low temperatures for both samples. This AFM ordering is also corroborated by the linear behaviour of M vs. H curves and by heat capacity measurements (not shown here). The increasing tendency of the magnetization at the lowest temperatures suggests the presence of a paramagnetic contribution, which should be related to small amounts of Ru ions not magnetically ordered or to extrinsic magnetic impurities at very low concentration (below the resolution of the XRD technique). Frequency-dependent (10 Hz–10 kHz) ac magnetic susceptibility measurements also show cusps at 12 and 47 K the positions which are frequency independent thus suggesting the absence of spin-glass or cluster-glass behaviour.

The PAC technique assesses time evolution of the γ emission of $^{111}\text{In} \rightarrow ^{111}\text{Cd}$ decay caused by the hyperfine interactions.

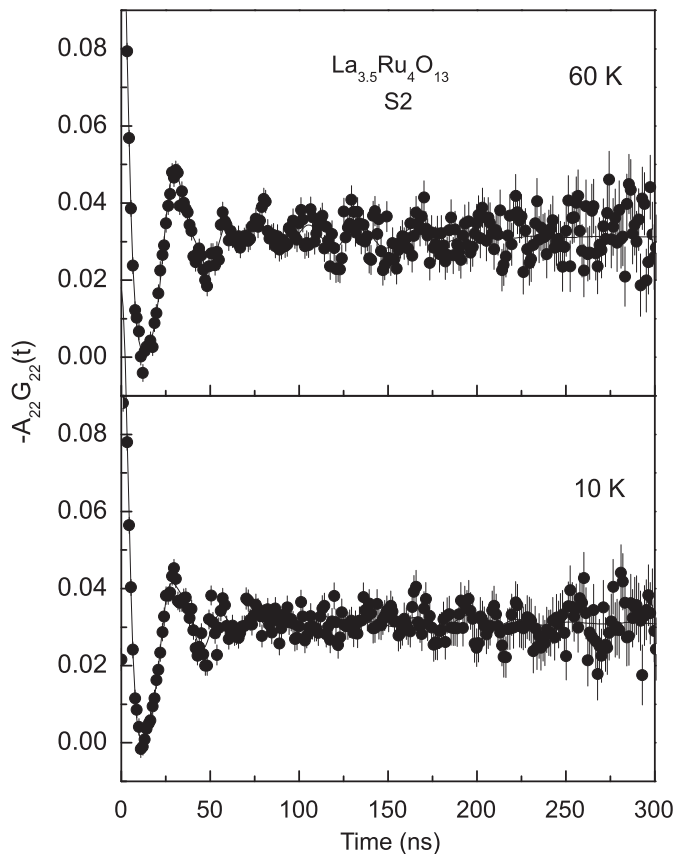


Fig. 3. Perturbation functions of the ^{111}Cd probe obtained at above and below T_N . The line represents the fit to the data.

The perturbation factor $G_{22}(t)$ contains detailed information about the Larmor and nuclear quadrupole frequency and asymmetric parameter. For detailed description of this technique, see for instance Ref. [12]. In contrast to magnetic measurements, no evidence of a magnetic ordering is determined from the analysis, since fits including magnetic contributions were not successful. However, PAC spectra were well-resolved considering only quadrupole interactions. The PAC spectra obtained at 60 K (see Fig. 3) was fitted with three nuclear quadrupole components. Based on previous reports of PAC measurements carried out in perovskite systems [12], we assigned the lower quadrupole frequency ($\nu_Q = 133$ MHz) to ^{111}Cd probe nuclei at Ru site and

the higher one ($\nu_Q = 206$ MHz) to the probe at La site. The third component, with intermediate frequency and with the lowest fraction (~ 0.10) is less resolved. The temperature dependence of the quadrupole frequency of ^{111}Cd probes at Ru and La sites shows a discontinuity at ~ 40 K near to the temperature associated to T_N (~ 47 K). Whereas the ν_Q at Ru site increases until $\nu_Q = 143$ MHz at $T = 10$ K, the ν_Q at La site shows opposite tendency as the temperature is decreased, becoming $\nu_Q = 161$ MHz at $T = 10$ K. The asymmetric parameter also shows a discontinuity for both sites at $T \sim 40$ K, which is more clearly observed for the ^{111}Cd probe at the site assigned to La ion. The increase of the asymmetric parameter from $\eta \sim 0.11$ (~ 0.76) for $T > 40$ K to ~ 0.46 (~ 0.81) in the low-temperature region for the site assigned to La (Ru) ion, indicates a structural distortion of the cation neighbourhood when the temperature is below $T < 40$ K.

In summary, polycrystalline $\text{La}_{3.5}\text{Ru}_4\text{O}_{13}$ compounds prepared under two different atmospheres has been studied. An electronic delocalization feature is suggested due to the relatively shorter Ru–O bond distances along the *rutile-like* slabs axis (*b*-axis) for both samples. The Curie–Weiss behaviour of the magnetic susceptibility provides an effective magnetic moment coherent with Ru ions in low-spin state ($S = 1/2$ and $S = 1$) and suggests the coexistence of Ru^{4+} and Ru^{3+} ions. ^{111}Cd -PAC measurements reveal non-magnetic, quadrupole interactions in the temperature range 10–60 K and indicate structural distortions when $T < 40$ K.

Acknowledgments

This work was supported by the Brazilian Science and Technology Ministry (MCT) and FINATEC. The authors thank E.M. Guimarães and O.F. de Lima for the XRD measurements and for helpful discussions.

References

- [1] Y. Maeno, et al., Nature 372 (1994) 532.
- [2] M.K. Crawford, et al., Phys. Rev. B 65 (2002) 214412.
- [3] P. Khalifah, et al., Nature 411 (2001) 669.
- [4] P. Khalifah, R.J. Cava, Phys. Rev. B 64 (2001) 085111.
- [5] P. Khalifah, et al., Science 297 (2002) 2237.
- [6] S.K. Malik, D.C. Kundaliya, R.D. Kale, Solid State Commun. 135 (2005) 166.
- [7] G. Cao, et al., Phys. Rev. B 56 (1997) R2916.
- [8] J.A.H. Coaquira, et al., J. Appl. Phys. 106 (2009) 013909.
- [9] F. Abraham, J. Trehoux, D. Thomas, J. Solid State Chem. 32 (1980) 151.
- [10] W.B. Yelon et al., to be published.
- [11] N.E. Brese, M. O'Keefe, Acta Cryst. B 47 (1991) 192.
- [12] R. Droga, et al., Phys. Rev. B 63 (2001) 224104.